

COHERENCE CHARACTERISTICS OF RADAR SIGNALS FROM ROUGH SOIL

X. Luo, J. Askne, G. Smith, and P. Dammert

Department of Radio and Space Science
Chalmers University of Technology
SE-41296, Göteborg, Sweden

Abstract—To understand the mechanisms of decorrelation in interferometric SAR (InSAR) images of bare soil, a model has been developed. Under the Kirchhoff and stationary phase approximations, coherence can be related to the statistical variations of dielectric constant and roughness parameters of surfaces. With the help of an empirical model for the dependence of dielectric constant on soil moisture, coherence due to the inhomogeneity of soil moisture is numerically demonstrated. It has been shown that the decorrelation of the radar signal from rough soil is mainly due to the moisture variability within the resolution cell. The effect of roughness on decorrelation is complex. The effect is negligible compared to that of the dielectric variability for homogeneous resolution cells (no dielectric variability within a resolution cell). However, the coherence depends strongly on the roughness parameters for resolution cells with large moisture variability. It is concluded that the loss of coherence induced by variability of dielectric constant can be related to the relative variation of moisture expressed by the ratio of standard deviation and mean value, and that large relative variations of moisture could lead to much decorrelation. If the moisture variability is small the coherence will be very high even if the values of mean moisture of the two SAR observations are different, which means that coherence can be high in spite of much backscatter differences.

1. Introduction

2. Theoretical Development

- 2.1 Coherence of Signals from Surfaces with Inhomogeneous Moisture Distribution within the Resolution Cell
- 2.2 Coherence of Signals from Surfaces with Homogeneous

Moisture within Resolution Cell

3. Results and Discussions

- 3.1 Effects of Soil Moisture Inhomogeneity within Resolution Cell
- 3.2 Effects of Soil Moisture Fluctuation between Resolution Cells
- 3.3 Roughness Effects

4. Conclusions

References

1. INTRODUCTION

Interferometric SAR (InSAR) is a powerful tool for mapping of land topography, detection of land change and potentially for the extraction of bio-physical parameters, e.g., stem volume of forest [1–3]. Much effort has been concentrated on understanding mechanisms causing decorrelation in InSAR and trying to relate the coherence to bio-physical parameters [4–9].

An important aspect for the interpretation of InSAR images is the coherence due to rough dielectric surfaces. Due to the lack of theoretical models differential simplified approaches have been used. For developing the simplified model for forest coherence in [5], the coherence due to soil was assumed to be unity, whereas, in [7], the ground coherence was an unknown value to be determined from measurements. To understand the properties of surface coherence, it is necessary to have physical insights into the mechanism of decorrelation due to rough surfaces. The effect of roughness on baseline decorrelation was studied in [10, 11], and an analytical expression for the coherence related to the roughness has been found under the physical optics (PO) approximation. It was demonstrated that the dependence of the baseline decorrelation on the surface statistics is weak for a wide range of values of the standard deviation and correlation length for the surfaces. Some experiments for investigating the decorrelation and phase shift of scattering from rough surfaces due to moisture changes were also made in laboratory [12, 13], where it was shown that changes in soil moisture caused decorrelation.

In this paper we analyze some factors that affect the coherence of radar signals backscattered from rough surfaces. The intention is to identify the most important factor causing decorrelation. Emphasis is placed on the effects of inhomogeneities of the surface dielectric prop-

erties within the resolution cell. In Section 2, a model is developed to relate coherence to the statistical characteristics of Fresnel reflection coefficient at normal incidence to the mean surface, and an analytical form of coherence in terms of roughness parameters is formulated under the Kirchhoff approximation (KA) with stationary phase approximation. In Section 3 results and discussions of the effects of the soil moisture in combination with roughness are presented. Conclusions are drawn in Section 4.

2. THEORETICAL DEVELOPMENT

2.1 Coherence of Signals from Surfaces with Inhomogeneous Moisture Distribution within the Resolution Cell

The size of the resolution cell for typical contemporary satellite SAR systems are tens of meters, for example, the value of ERS-1/2 is about 25 meters. Thus it is likely that the soil moisture (and other properties) varies even within the resolution cell. In this section, an expression for coherence is developed including the moisture variability within the resolution cell. As illustrated in Figure 1(a), the resolution cell can be divided into M sub-cells with the centers located at (x_i, y_i) , where the index i ranges from 1 to M . For each subcell, the roughness properties are assumed statistically identical, but dielectric properties may be different. The total field E^s is the summation of each subcell's contribution E_i .

$$E^s = \sum_{i=1}^M E_i \quad (1)$$

Under the tangent plane approximation with the stationary phase approximation, the backscattered electric field E_i from the i th subcell for co-polarizations (vertical and horizontal) can be expressed as [14]

$$E_i = KI_i E_0 R_i(0) \quad (2)$$

Where

$$R_i(0) = (\sqrt{\varepsilon_i} - \sqrt{\varepsilon_0}) / (\sqrt{\varepsilon_i} + \sqrt{\varepsilon_0}) \quad (3)$$

$$I_i = q/|q_z| \int_{\Delta_i} \exp[-j2k\hat{n}_i \cdot \vec{r}] dx dy \quad (4)$$

$$K = jk \exp(-jkR_0)/4\pi R_0 \quad (5)$$

$$q = |-2k\hat{n}_i| \equiv |q_x \hat{x} + q_y \hat{y} + q_z \hat{z}| \quad (6)$$

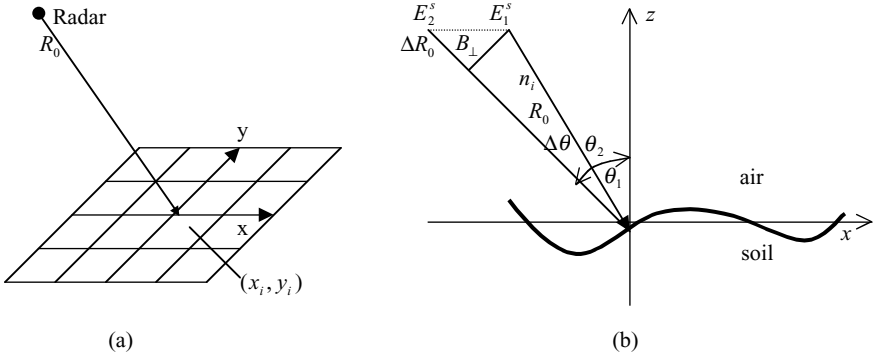


Figure 1. (a) Illustrates a resolution cell with inhomogeneous moisture can be further divided into several subcells, (b) shows the InSAR geometry.

And \hat{n}_i is the unit vector in the incident direction with angle θ , k is the wave number in air, E_0 is the amplitude of the incident field and R_0 is the range from the observation point to the rough surface (see Figure 1(b)). \vec{r} represents the position of a point on the surface from the origin. ε_0 and ε_i are relative dielectric constants for air and soil of the i th subcell, respectively, and $R_i(0)$ is the Fresnel reflection coefficient at normal incidence. The integration is carried out in the subcell Δ_i . The validity conditions for Eq. (2) for a Gaussian rough surface with Gaussian correlation function are given in Eq. (33) and (34). Here we assume that the impulse function of SAR system is a rectangular window. Then the total field from a resolution cell can be presented as

$$E^s = KE_0q/|q_z| \sum_{i=1}^M R_i(0)G_i \quad (7)$$

Where

$$G_i = \int_{\Delta_i} \exp[-j2k\hat{n}_i \cdot \vec{r}] dx dy \quad (8)$$

The coherence of two observed fields E_1^s and E_2^s with slightly different incidence angles θ_1 and θ_2 , respectively, is defined as [1]

$$r = \langle E_1^s E_2^{s*} \rangle / \sqrt{\langle |E_1^s|^2 \rangle \langle |E_2^s|^2 \rangle} \quad (9)$$

The operation $\langle \cdot \rangle$ denotes the ensemble average. The statistical variations include both spatial variations between pixels and time variations

for repeat pass interferometry, and the asterisk ‘*’ represents the complex conjugate operation. The simple geometry of InSAR is depicted in Figure 1(b). The quantities with subscript ‘1’ are for one image, and those with subscript ‘2’ correspond to another one taken at a position with a baseline B_{\perp} perpendicular to the average look direction. When considering the range difference ΔR_0 between the two observations, the above expression can be rewritten as

$$r = \exp(j2k\Delta R_0)B_{12}/\sqrt{B_{11}B_{22}} \quad (10)$$

Where

$$B_{ab} = \left\langle \sum_{m=1}^M \sum_{n=1}^M R_{am}(0)R_{bn}^*(0)G_{am}G_{bn}^* \right\rangle, \quad ab = 11, 12, 22 \quad (11)$$

For simplicity, the phase term $\exp(j2k\Delta R_0)$ that corresponds to coherent phase shift, will be ignored in the following discussion where we focus on the magnitude of the coherence. Now we calculate the term B_{ab} . If the moisture and the roughness are independent of each other, the ensemble averaging can be done for moisture and roughness separately, and Eq. (11) can be divided into two terms corresponding to the correlation for the same subcell and different ones, respectively.

$$\begin{aligned} B_{ab} &= \sum_{m=1}^M \langle R_{am}(0)R_{bm}^*(0) \rangle \langle G_{am}G_{bm}^* \rangle \\ &+ \sum_{m=1}^M \sum_{n=1, n \neq m}^M \langle R_{am}(0)R_{bn}^*(0) \rangle \langle G_{am}G_{bn}^* \rangle \end{aligned} \quad (12)$$

For simplicity, we can assume the incidence direction is $\hat{n}_i = \hat{x} \sin \theta - \hat{z} \cos \theta$. The ensemble average for the roughness in the same subcell can be described as

$$\begin{aligned} C_{ab} &= \langle G_{am}G_{bm}^* \rangle \\ &= \iint_{\Delta m \Delta m} \exp[-j(k_{xa}x_1 - k_{xb}x_2)] \langle \exp(jk_{za}z_1 - jk_{zb}z_2) \rangle dx_1 dy_1 dx_2 dy_2 \\ &= \iint_{\Delta m \Delta m} \exp[-j(k_{xa}x_1 - k_{xb}x_2)] \\ &\quad \cdot \exp[-(k_{za}^2 + k_{zb}^2) \sigma^2/2 + \sigma^2 k_{za} k_{zb} \rho(\tau)] dx_1 dy_1 dx_2 dy_2 \end{aligned} \quad (13)$$

Where

$$k_{xa} = 2k \sin \theta_a, \quad k_{za} = 2k \cos \theta_a, \quad a = 1, 2 \quad (14)$$

And σ is the standard deviation of the surface. $\rho(\tau)$ is the correlation function of the rough surface height, τ is the distance of two points on the surface, that is $\tau = \sqrt{(x_2 - x_1)^2 + (y_2 - y_1)^2}$. The term involving $\rho(\tau)$ may be represented by a series, so Eq. (13) becomes a series,

$$C_{ab} = \exp \left[- (k_{za}^2 + k_{zb}^2) \sigma^2 / 2 \right] \int \int_{\Delta m \Delta m} \exp[-j(k_{xa}x_1 - k_{xb}x_2)] \cdot \left\{ 1 + \sum_{n=1}^{\infty} \frac{(\sigma^2 k_{za} k_{zb} \rho(\tau))^n}{n!} \right\} dx_1 dy_1 dx_2 dy_2 \quad (15)$$

It is shown that the first term corresponds to the coherent scattering, the second term corresponds to the incoherent scattering. These two scattering mechanisms can be calculated separately. The coherent term is

$$C_{ab}^c = A^2 \exp \left[- (k_{za}^2 + k_{zb}^2) \sigma^2 / 2 \right] \text{sinc}(k_{xa}L_x) \text{sinc}(k_{xb}L_x) \cdot \exp(-j(k_{xa} - k_{xb})x_m) \quad (16)$$

Where $2L_x$ and $2L_y$ are the size of subcell in x and y directions respectively. A is the area of the subcell, i.e., $A = 4L_xL_y$ and $\text{sinc}(x) = \sin x/x$.

For Gaussian height correlation function, $\rho(\tau) = \exp(-\tau^2/l^2)$, where l is the correlation length, following the same coordinate transform as [10, 11, 15], the incoherent scattering is further presented as

$$\begin{aligned} C_{ab}^i &\approx \exp \left[- (k_{za}^2 + k_{zb}^2) \sigma^2 / 2 \right] \int_{x_m - L_x}^{x_m + L_x} \int_{y_m - L_y}^{y_m + L_y} \exp[-j(k_{xa} - k_{xb})x] dy dx \\ &\cdot \sum_{n=1}^{\infty} \frac{(\sigma^2 k_{za} k_{zb})^n}{n!} \int_0^{\infty} \int_0^{2\pi} \exp(-j(k_{xa} + k_{xb})\tau \cos \varphi / 2) \\ &\cdot \exp(-n\tau^2/l^2) \tau d\tau d\varphi \\ &= A\pi \exp \left[- (k_{za}^2 + k_{zb}^2) \sigma^2 / 2 \right] \text{sinc}[(k_{xa} - k_{xb})L_x] \exp(-j(k_{xa} - k_{xb})x_m) \\ &\cdot \sum_{n=1}^{\infty} \frac{(\sigma^2 k_{za} k_{zb})^n}{n!n} \exp[-l^2(k_{xa} + k_{xb})^2 / (16n)] \end{aligned} \quad (17)$$

When $k\sigma \gg 1$, the contribution of the integral in (13) is significant only for small values of τ , so the correlation function may be approximated as $\rho(\tau) \approx 1 - \tau^2/l^2$. Then with the same procedure as applied in (17), we can obtain the approximate expression

$$C_{ab} \approx \pi Al^2 \exp[-j(k_{xa} - k_{xb})x_m] \frac{\text{sinc}[(k_{xa} - k_{xb})L_x]}{k_{za}k_{zb}\sigma^2} \cdot \exp\left[\frac{-(k_{za} - k_{zb})^2\sigma^2}{2} - \frac{(k_{xa} + k_{xb})^2l^2}{16k_{za}k_{zb}\sigma^2}\right] \quad (18)$$

For the integral over two different subcells, D_{ab} , we can assume the roughness is independent, and we can derive

$$\begin{aligned} D_{ab} &= \langle G_{am}G_{bn}^* \rangle \\ &= \exp[-(k_{za}^2 + k_{zb}^2)\sigma^2/2] \\ &\quad \cdot \int_{\Delta_m} \exp(-jk_{xa}x_1)dx_1dy_1 \int_{\Delta_n} \exp(jk_{xb}x_2)dx_2dy_2 \\ &= A^2 \exp[-(k_{za}^2 + k_{zb}^2)\sigma^2/2] \text{sinc}(k_{xa}L_x)\text{sinc}(k_{xb}L_x) \\ &\quad \cdot \exp(-j(k_{xa}x_m - k_{xb}x_n)) \end{aligned} \quad (19)$$

Hence, B_{ab} can be derived

$$\begin{aligned} B_{ab} &= \sum_{m=1}^M \langle R_{am}(0)R_{bm}^*(0) \rangle (C_{ab}^c + C_{ab}^{nc}) \\ &\quad + \sum_{m=1}^M \sum_{n=1, n \neq m}^M \langle R_{am}(0)R_{bn}^*(0) \rangle D_{ab} \end{aligned} \quad (20)$$

When $k\sigma \gg 1$, C_{ab} is calculated through Eq. (18).

Now we discuss the statistics of moisture distribution. If the moistures for all subcells are statistically identical, we can rewrite the above expression.

$$B_{ab} = \langle R_a(0)R_b^*(0) \rangle^s \sum_{m=1}^M (C_{ab}^c + C_{ab}^i) + \langle R_a(0)R_b^*(0) \rangle^d \sum_{m=1}^M \sum_{n=1, n \neq m}^M D_{ab} \quad (21)$$

Where $R_1(0)$ and $R_2(0)$, which are the Fresnel coefficients for the two observations, are random variables. The superscripts 's' and 'd'

denote the operations of ensemble averaging which are carried out on the same subcell and on different subcells respectively.

If we only consider the decorrelation due to the rough surface, we set $\theta_1 = \theta_2 = \theta$, as the case shown in [12, 13], B_{ab} is simplified as

$$B_{12} = \langle R_1(0)R_2^*(0) \rangle^s C_0 + \langle R_1(0)R_2^*(0) \rangle^d D_0 \quad (22a)$$

$$B_{11} = \langle |R_1(0)|^2 \rangle C_0 + \langle R_1(0)R_1^*(0) \rangle^d D_0 \quad (22b)$$

$$B_{22} = \langle |R_2(0)|^2 \rangle C_0 + \langle R_2(0)R_2^*(0) \rangle^d D_0 \quad (22c)$$

Where C_0 and D_0 are given as

$$C_0 = M \exp(- (2k\sigma \cos \theta)^2) \left\{ A^2 \text{sinc}^2(2kL_x \sin \theta) + A\pi l^2 \sum_{n=1}^{\infty} \frac{(2k\sigma \cos \theta)^{2n}}{n!n} \exp\left[-\frac{(kl \sin \theta)^2}{n}\right] \right\} \quad (23)$$

$$D_0 = \exp(- (2k\sigma \cos \theta)^2) A^2 \text{sinc}^2(2kL_x \sin \theta) \cdot \sum_{m=1}^M \sum_{n=1, n \neq m}^M \exp[-j2k \sin \theta (x_m - x_n)] \quad (24)$$

So for the single pass case $B_{12} = B_{11} = B_{22}$. For $k\sigma \gg 1$, C_0 is expressed as

$$C_0 = \pi M A l^2 / (2k\sigma \cos \theta)^2 \exp[-(l \tan \theta)^2 / (2\sigma)^2] \quad (25)$$

So far we have derived theoretical expressions for coherence for the case of inhomogeneous resolution cell. For large roughness only incoherent scattering contributes to coherence, and for smaller roughness, both coherent and incoherent scattering make contributions to the coherence of rough soil. In the following subsection, we will discuss the special case in which there is no moisture variability within a resolution cell.

2.2 Coherence of Signals from Surfaces with Homogenous Moisture within Resolution Cell

We now assume that the moisture in resolution cell is homogenous, i.e., the number of subcells is one. We also assume that the center of

resolution cell is located at the origin. From (9)–(12), the expression of coherence can be presented as

$$r = \frac{C_{12}}{\sqrt{C_{11}C_{22}}} \frac{\langle R_1(0)R_2^*(0) \rangle}{\sqrt{\langle |R_1(0)|^2 \rangle \langle |R_2(0)|^2 \rangle}} \quad (26)$$

Where C_{ab} is calculated through Eq. (13). Here we just show various effects on the coherence in the case of large $k\sigma$, the same procedure could be applied for the case of small $k\sigma$.

With $x_m = 0$ in (18), we can derive C_{ab} for large values of $k\sigma$. The coherence can be separated into three terms,

$$r = r_m r_B r_r \quad (27)$$

$$r_m = \langle R_1(0)R_2^*(0) \rangle / \sqrt{\langle |R_1(0)|^2 \rangle \langle |R_2(0)|^2 \rangle} \quad (28)$$

$$r_r \approx \exp \left[-2(k\sigma)^2 (\cos \theta_2 - \cos \theta_1)^2 \right] \cdot \exp \left[-\frac{(\sin \theta_1 + \sin \theta_2)^2 l^2}{16 \cos \theta_1 \cos \theta_2 \sigma^2} + \frac{l^2 (\tan^2 \theta_1 + \tan^2 \theta_2)}{8\sigma^2} \right] \quad (29)$$

$$r_B = \text{sinc} [2k(\sin \theta_1 - \sin \theta_2)L_x] \quad (30)$$

r_m represents the coherence due to the fluctuation of dielectric properties, for example, variation of soil moisture or inhomogeneity of soil composition. r_r shows the coherence due to the surface roughness which can be characterized by the parameters, e.g., RMS height, σ , and correlation length, l . The baseline coherence r_B represents the baseline decorrelation due to the spatial diversity of radar positions where two images are derived, it is independent of the surface properties, and determined by the impulse function of SAR systems. The form of comes from the rectangular impulse function of SAR system. Baseline decorrelation for some typical impulse functions has been discussed in references, the sinc form in [6, 9, 11], Gaussian function in [15], and the so-called ‘cosine on a pedestal’ impulse function in spatial frequency in [16].

Trigonometric functions of θ_2 in (29) and (30) can be expressed in terms of θ_1 and the angle difference $\Delta\theta$. We use θ to represent θ_1 for simplicity. Using the approximations $\cos(\Delta\theta) \approx 1$, $\sin(\Delta\theta) \approx \Delta\theta$, neglecting terms higher than second order of $\Delta\theta$, and expressing $\Delta\theta$ with the baseline orthogonal to the sight direction approximately, that

is, $\Delta\theta \approx B_{\perp}/R$, r_r and r_b may be further expressed approximately as

$$r_r \approx \exp \left[-2(k\sigma B_{\perp} \sin \theta)^2 / R_0^2 \right] \cdot \exp \left[(lB_{\perp} / (4\sigma R_0))^2 (2 \tan^4 \theta + 4 \tan^2 \theta + 1) \right] \quad (31)$$

$$r_B = \text{sinc}[(k\Delta r B_{\perp}) / (R_0 \tan \theta)] \quad (32)$$

Where Δr is the resolution size in the range direction, B_{\perp} is the baseline orthogonal to the sight direction.

For the Gaussian rough surface with Gaussian correlation function, the conditions for the validity of the coherence expressions are the same as the backscattering case [14]. For the tangent plane approximation, the following condition should be satisfied.

$$kl > 6, \quad l^2 > 2.76\sigma\lambda \quad (33)$$

Where λ is the wavelength in the free space. And for the case of large values of $k\sigma$, an additional condition is required, i.e.,

$$(q_z\sigma)^2 > 10 \quad (34)$$

Thus, we have shown how the coherence of radar signals from rough surface can be explicitly presented in terms of Fresnel reflection coefficient at normal incidence to the mean surface and roughness parameters of RMS height and correlation length.

3. RESULTS AND DISCUSSIONS

3.1 Effects of Soil Moisture Inhomogeneity within Resolution Cell

In Section 2, the coherence due to the dielectric properties of the surface is related to the statistical characteristics of Fresnel reflection coefficients, thus related to the statistical properties of the dielectric constant of the surface. Here we only study the effect of moisture. The soil composition (in terms of percentage of clay, sand and silt) is fixed, so the dielectric constant of soil is related to soil moisture and soil temperature. If the soil moisture is homogenous, even though the two states of moisture, where images are derived, may differ a lot, and the backscattering may show large differences (such a case has been observed, see [3]), there is no expected decorrelation. That is, it is the inhomogeneity of the surface's dielectric properties that induces the

decorrelation of the backscattered signal, not the difference of dielectric properties of two soil states, although the difference will contribute to the phase shift.

The dielectric constant of soils may be related to the content and moisture through well-known empirical models [17]. Generally we do not know much about the statistical characteristics of soil moisture, especially the spatial and temporal correlation of soil moisture on the small-scales of relevance here. We assume that soil moisture (volumetric moisture) is an independent Gaussian random variable defined by its mean value μ_m and standard deviation (RMS) σ_m . The assumption of statistical independence of moisture will induce overestimation of decorrelation to some degree, but we can have physical insight into the decorrelation mechanism with this simple assumption. Therefore the probability distribution function of moisture within different subcells is assumed to be

$$p(m_v) = \left[1 / \left(\sqrt{2\pi}\sigma_m \right) \right] \exp \left[-(m_v - \mu_m)^2 / (2\sigma_m^2) \right] \quad (35)$$

where m_v is the volumetric moisture.

The dielectric constant of soil is expressed as a polynomial of volumetric moisture, that is

$$\varepsilon = (a_0 + a_1S + a_2C) + (b_0 + b_1S + b_2C)m_v + (c_0 + c_1S + c_2C)m_v^2 \quad (36)$$

Where ε is the relative dielectric constant of the soil, S and C are the fractions of sand and clay in the soil (the remainder assumed to be silt), and coefficients a_i , b_i , c_i ($i = 1, 2, 3$) are functions of frequency [17].

From Eqs. (22)–(24), it is clear that effects of roughness and moisture are coupled. For large values of $k\sigma$, the term D_0 between different subcells shown in Eq. (24) is very small compared to the term C_0 in Eq. (25), so the total coherence is only determined by the fluctuations of Fresnel reflection coefficient, the effects of roughness disappear, in this case the value of coherence will be the maximum, that is,

$$r_{\max} = \langle R_1(0)R_2^*(0) \rangle / \sqrt{\langle |R_1(0)|^2 \rangle \langle |R_2(0)|^2 \rangle} \quad (37)$$

The coherence of radar signals for inhomogeneous resolution cells behaves like that of signals from homogeneous resolution cells. The value of coherence is high, as will be shown in next subsection. For smaller

values of $k\sigma$ and correlation length l , the term C_0 in Eq. (23) is still much larger than the term D_0 in (24), this is the same situation as the case of large $k\sigma$. When the correlation length becomes larger, the incoherent scattering from a subcell decreases, and the coherent scattering, the first term in (23), dominates, the interference between subcells becomes more important. When incoherent scattering vanishes, that is, the second term of (23) is approaching to zero, the total field is largely affected by the phase differences due to the position differences of subcells, and we get the maximum decorrelation. In this case the coherence is strongly affected by the moisture variability within the resolution cell through the propagation phase differences, as shown in (39). The coherence can be expressed as

$$r_{\min} = \frac{\{M + M_1\} \langle R_1(0)R_2^*(0) \rangle}{\left\{ \begin{aligned} & \left[M \langle |R_1(0)|^2 \rangle + M_1 \langle R_1(0)R_1^*(0) \rangle^d \right] \\ & \times \left[M \langle |R_2(0)|^2 \rangle + M_1 \langle R_2(0)R_2^*(0) \rangle^d \right] \end{aligned} \right\}^{1/2}} \quad (38)$$

where

$$M_1 = \sum_{m=1}^M \sum_{n=1, n \neq m}^M \exp[-j2k \sin \theta (x_m - x_n)] \quad (39)$$

This result can be interpreted by regarding each subcell as a point scatterer with an amplitude proportional to the Fresnel reflection coefficient, and with the phase center located at the geometrical center of the subcell. In Eq. (2), if the surface height z is zero, the field from a resolution cell may be expressed as

$$E_a^s = \sum_{m=1}^M C_1 R_a(0) \exp(-j2k \sin \theta x_m), \quad a = 1, 2 \quad (40)$$

Where C_1 is a constant that includes the contribution of the size of subcell, space spread factor etc., shown in (2). The total coherence will be in the range:

$$|r_{\min}| \leq |r| \leq |r_{\max}| \quad (41)$$

The coherence due to moisture has been estimated by numerical simulation using randomly generated values of soil moisture. As an example, one class of soil with sand fraction 0.5 and clay fraction 0.2 was considered. In the simulation of this paper we assume that there are 10 subcells in x direction in one resolution cell. ERS SAR is used

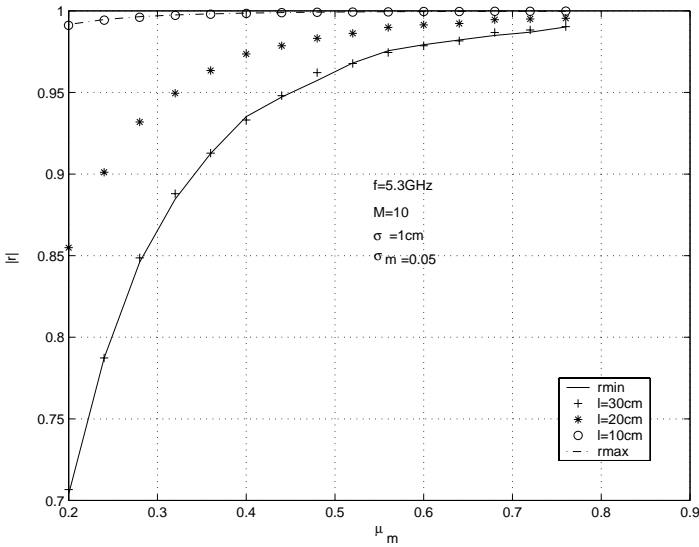


Figure 2. Showing how coherence varies when the mean value of the soil moisture changes for a small value of $k\sigma$. The moisture variability in the resolution cell is fixed (RMS variation of 5% volumetric moisture content), and the soil moisture for two images has the same statistical properties.

as an example with the following parameters: incidence angle: 23 degrees, range: 850 km, frequency: 5.3 GHz, and frequency bandwidth: 15.5 MHz. The size of a resolution cell is 25 meters both in azimuth and range directions.

In Figure 2, the coherence variation with mean soil moisture is illustrated with different values of surface correlation length, for small value of roughness σ . The maximum and minimum limits of coherence are also shown. The states of the soil are statistically identical for the two observations. Given the standard deviation of moisture, σ_m , the coherence increases with increasing moisture. With increasing correlation length, coherence decreases, and reaches the minimum limit very quickly, where coherent scattering dominates. In Figure 3, the coherence variation with mean soil moisture is shown for large roughness σ . The values of coherence are always large, and are independent of the correlation length. The coherence is only determined by the statistics of the soil's dielectric properties. The variation of coherence with standard deviation of soil moisture is depicted in Figure 4, for fixed mean values of soil moisture. The coherence decreases when the

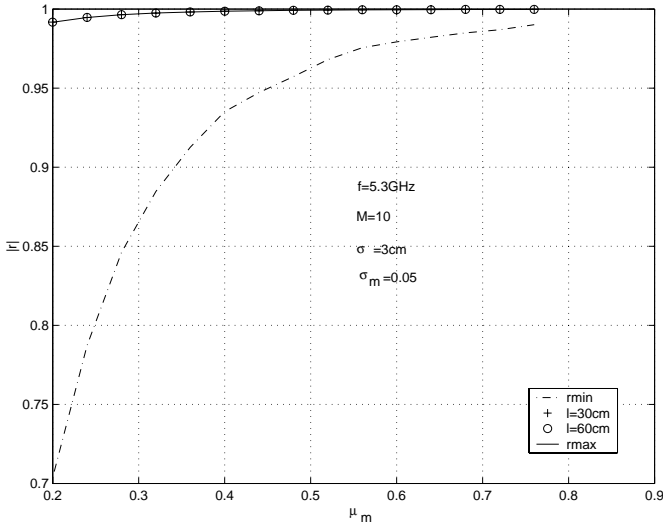


Figure 3. Showing how coherence varies when the mean value of the soil moisture changes for large value of $k\sigma$. The moisture variability in the resolution cell is fixed (RMS variation of 5% volumetric moisture content), and the soil moisture for two images has the same statistical properties.

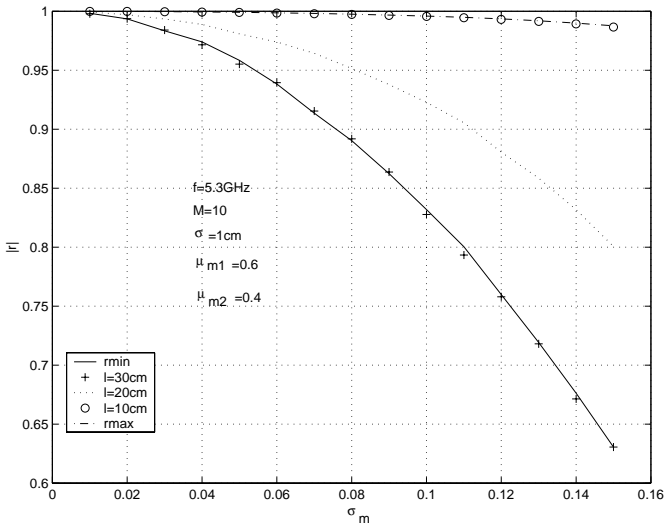


Figure 4. Showing the dependence of coherence on variability of standard deviation of moisture for a small value of $k\sigma$. The variability of soil moisture exists within the resolution cell with a fixed RMS variation, but with different mean values.

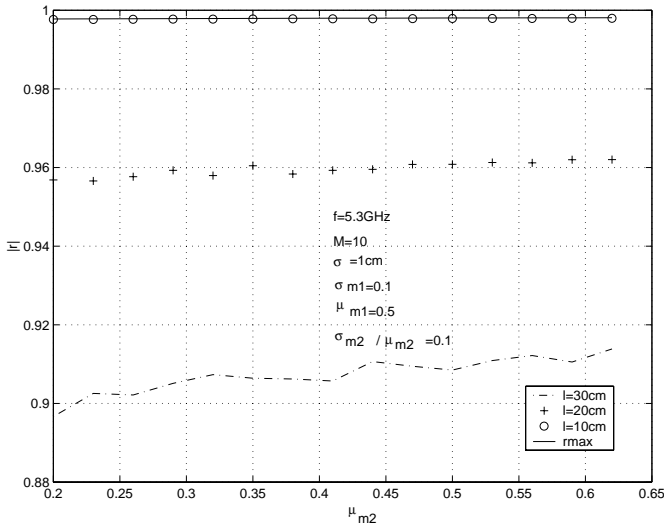


Figure 5. Showing how coherence for a fixed ratio of soil moisture standard deviation to mean value varies with the mean moisture content of the second image. Soil moisture is variable within the resolution cell.

standard deviation of moisture increases. It seems as if the coherence changes with the relative variation of moisture. Thus in Figure 5, coherence variation with mean moisture is demonstrated for a fixed ratio of the standard deviation to the mean value for the second image, that is, keeping the relative variation constant. Coherence changes slowly with the increase of mean moisture for all cases of roughness. It is clear that the coherence depends on the relative fluctuation of soil moisture.

3.2 Effects of Soil Moisture Fluctuation between Resolution Cells

If the soil moisture is homogeneous within the resolution cell, effects of soil roughness and moisture are de-coupled. So we can consider the two effects separately. The roughness effects on coherence will be discussed in the next subsection. The coherence variation with the mean moisture of the second image is presented in Figure 6, where the frequency dependence is also shown. The same behavior of coherence change with moisture as illustrated previously is shown. The coherence is high. We can find that the frequency dependence of coherence is complex because of the non-linear relationship between the Fresnel

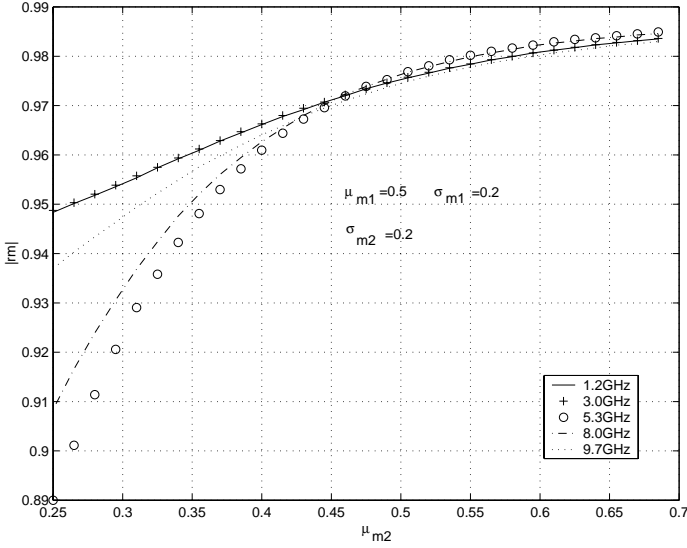


Figure 6. Showing the dependence of coherence r_m on variability of soil moisture of the second image for different frequencies. No moisture variability exists within the resolution cell.

coefficient and the moisture. It is shown that radar signals from soil surface may have very high correlation despite large changes of soil moisture.

3.3 Roughness Effects

For inhomogeneous resolution cells, the effects of roughness have been discussed in Section 3.1.

When roughness is small, the effect of phase differences due to the position differences for different subcells becomes more important, thus signals maybe largely decorrelated due to the moisture variability within a resolution cell. When roughness is large, the effect of phase differences due to the position differences is taken over by that of roughness, in this case, the coherence of signal is mainly determined by the fluctuation of Fresnel reflection coefficient, thus high coherence may be observed.

For homogeneous resolution cells, the relation of coherence and roughness is expressed in Eq. (31). For ERS SAR the dependence of coherence on variations of the correlation length and RMS height of the surface are presented in Figure 7 and Figure 8 for different base-

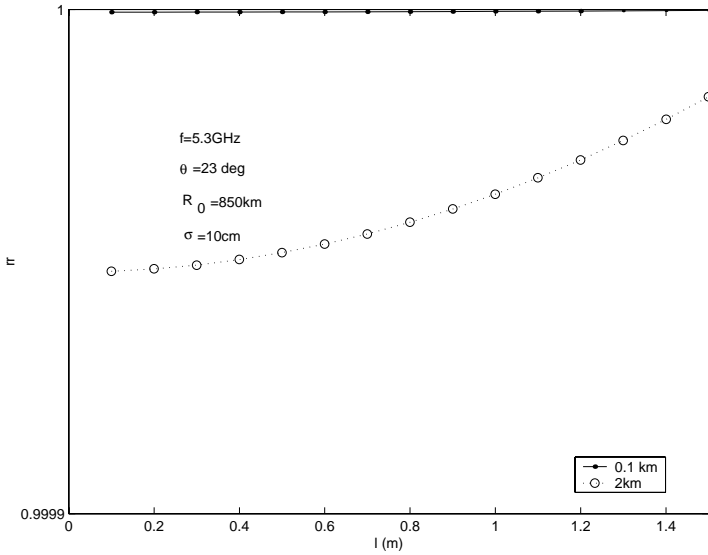


Figure 7. Illustrating the dependence of coherence r_r on surface height correlation l for the case of large $k\sigma$ and for different base-lines. Moisture within the resolution cell is homogeneous.

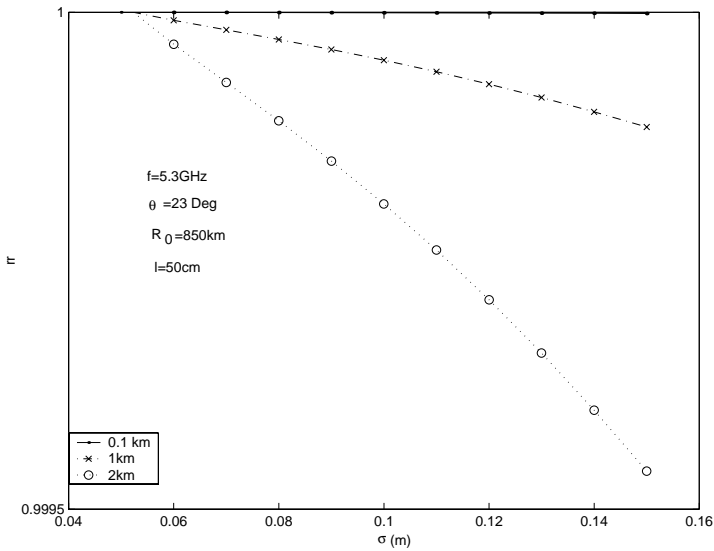


Figure 8. Illustrating the dependence of coherence r_r on RMS of surface height for the case of large $k\sigma$. The moisture is homogenous within the resolution cell.

lines, respectively. The numbers shown in the legend boxes are the values of the baseline orthogonal to the sight direction. In Figure 7, it appears that coherence increases with increasing correlation length, and coherence is almost one even for large baselines. In Figure 8, the decorrelation increases when RMS height becomes larger, especially for longer baselines. The effect of roughness for the case of homogeneous resolution cells is much different from that for the inhomogeneous case. The overall effect of roughness on coherence is much smaller than that of dielectric inhomogeneity.

4. CONCLUSIONS

Based on the Kirchhoff approximation under the stationary phase approximation, the coherence of the backscattered signal from a rough surface with inhomogeneous moisture distribution has been related to the statistical properties of dielectric and geometrical characteristics of the rough surface. Coherence due to the moisture inhomogeneity, roughness, and baseline has been explicitly given. With the assumption of statistical independence of soil moisture, coherence due to the surface's dielectric properties has been numerically calculated. Some conclusions can be drawn as follows.

The surface roughness effects are complex. Roughness strongly affects the coherence when the dielectric constant within a resolution cell is inhomogeneous. Only when the roughness is small the effect of moisture variability within a resolution cell on coherence can be obvious. However the effect of roughness on coherence turns out to be small when the roughness is very large, the coherence is determined by the fluctuation of Fresnel coefficient. The effect of roughness is so small that it may be negligible compared with that of dielectric properties for homogeneous resolution cells.

Signals from resolution cells with inhomogeneous moisture distribution will be much decorrelated when coherent scattering in a subcell dominates, where the interference between subcells due to the position differences of subcells is large. In such cases the variability of dielectric constant within a resolution cell is the main reason for signal decorrelation. Coherence is closely related to the relative variation of the dielectric constant, for a given soil composition, hence related to the relative variation of moisture expressed by the ratio of standard deviation to mean value. Large relative variations of moisture result in large decorrelation. If the moisture variability is small the coherence

will be very high even if the values of mean moisture of the two SAR observations are different, which means that coherence can be high in spite of much backscatter differences.

REFERENCES

1. Dammert, P. B. G., "Spaceborne SAR interferometry: Theory and applications," Technical Report No. 382, ISBN 91-7197-851-8, School of Electrical and Computer Engineering, Chalmers University of Technology, Gothenburg, Sweden, 1999.
2. Gens, R. and J. L. Van Genderen, Review article: "SAR interferometry-issues, techniques, applications," *International Journal of Remote Sensing*, Vol. 17, 1803–1835, 1996.
3. Hagberg, J. O., L. M. H. Ulander, and J. Askne, "Repeat pass SAR interferometry over forested terrain," *IEEE Trans. Geosci. Remote Sensing*, Vol. 33, 331–340, 1995.
4. Askne, J., P. B. G. Dammert, and G. Smith, "Understanding ERS InSAR coherence of boreal forests," *IGARSS'99*, 2111–2114.
5. Floury, N., T. L. Toan, J. C. Souyris, and J. Bruniquel, "A study of SAR interferometry over forests: theory and experiment," *IGARSS'97*, 1868–1870.
6. Rodriguez, E. and J. M. Martin, "Theory and design of interferometric synthetic aperture radars," *IEE Proc-F*, Vol. 139, No. 2, April 1992.
7. Smith, G., P. B. G. Dammert, and J. I. H. Askne, "Decorrelation mechanisms in C-band SAR interferometry over boreal forest," *Microwave Sensing and Synthetic Aperture Radar*, G. Franceschetti, C. J. Oliver, F. S. Rubertone, and S. Tajbakhsh, Editors, *Proceedings of SPIE*, Vol. 2958, 300–310, 1996.
8. Treuhaft, R. N., S. N. Madsen, M. Moghaddam, and J. J. van Zyl, "Vegetation characteristics and surface topography from interferometric radar," *Radio Science*, Vol. 31, 1449–1485, 1996.
9. Zebker, H. A. and J. Villasenzo, "Decorrelation in interferometric radar echoes," *IEEE Trans. Geosci. Remote Sensing*, Vol. 30, No. 5, Sept. 1992.
10. Franceschetti, G., A. Lodice, M. Migliaccio, and D. Riccio, "On the baseline decorrelation," *IGARSS'96*, 680–682.
11. Franceschetti, G., A. Lodice, M. Migliaccio, and D. Riccio, "The effect of surface scattering on IFSAR baseline decorrelation," *J. Electromagnetic Waves & Applications*, Vol. 11, 353–370, 1997.
12. Nesti, G., D. Tarchi, and J. P. Rudant, "Decorrelation of backscattered signal due to soil moisture changes," *IGARSS'95*, 2026–2028.

13. Nesti, G., D. Tarchi, D. Despan, J. P. Rudant, A. Bedidi, P. Borderies, and E. Bachelier, "Phase shift and decorrelation of radar signal related to soil moisture changes," *Proc. of the 2nd International Workshop on Retrieval of Bio- & Geo-Physical Parameter from SAR Data for Land Applications*, ESTEC, Noordwijk, The Netherlands, October 21–23, 1998. (ESA SP-441, 423–430, December 1998)
14. Ulaby, F. T., R. K. Moore, and A. K. Fung, *Microwave Remote Sensing, Active and Passive*, Vol. 2, 931, Addison-Wesley Publishing Company, 1982.
15. Le, C., Y. Kuga, and A. Ishimaru, "Angular correlation function based on the second-order Kirchhoff approximation and comparison with experiments," *J. Opt. Soc. Am. A*, Vol. 13, No. 5, 1996.
16. Ulander, L. M. H. and J. O. Hagberg, "Radiometric and interferometric calibration of ENVISAT-1 ASAR," Research Report No. 172, Department of Radio and Space Science with Onsala Space Observatory, Chalmers University of Technology, Gothenburg, Sweden, 1995.
17. Hallikainen, M., F. T. Ulaby, M. C. Dobson, M. El-Rayes, and L. K. Wu, "Microwave dielectric behavior of wet soil—Part I: Empirical models and experimental observations," *IEEE Trans. Geosci. Remote Sensing*, GE-23, 25–34.